Closed-Shell Ion Pair Structure and Dynamics: Steady-State $^1H\{^1H\}$, $^{10}B\{^1H\}$, and $^{11}B\{^1H\}$ Nuclear Overhauser Effects and ^{10}B, ^{11}B Nuclear Relaxation of Tetraalkylammonium Tetrahydridoborates in Ion-Pairing and Dissociative Solvents

Thomas C. Pochapsky,* An-Ping Wang, and Patricia M. Stone†

Contribution from the Department of Chemistry, Brandeis University, Waltham, Massachusetts 02254

Received June 4, 1993⊛

Abstract: The magnitudes of selective steady-state $^1H\{^1H\}$ interionic nuclear Overhauser effects (NOEs) and nonselective $^{10}B\{^1H\}$ and $^{11}B\{^1H\}$ NOEs as well as ^{10}B and ^{11}B spin–lattice relaxation times were measured for solutions of $(butyl)_4N^+,BH_4^-$ **1a** in $^2HCCl_3$, ^2H_2O, and $[^2H_6]$dimethyl sulfoxide. Interionic NOEs resulting from the selective saturation of cationic alkyl resonances were used to evaluate the time average structure of the ion pair **1a** in various solvents. The largest NOEs are observed in $^2HCCl_3$, while smaller specific interionic NOEs were observed in $[^2H_6]$-dimethyl sulfoxide and $[^2H_6]$benzene. Only small nonspecific interionic NOEs were observed in ^2H_2O solutions of **1a**. ^{10}B and ^{11}B T_1 relaxation times and nonselective steady-state $^{10}B\{^1H\}$ and $^{11}B\{^1H\}$ NOEs were also measured for solutions of $NaBH_4$ **2** in ^2H_2O and $[^2H_6]$dimethyl sulfoxide in order to determine the effect of counterion on observed relaxation behavior for BH_4^-. Dipolar and quadrupolar contributions to observed spin–lattice relaxation of both boron nuclei were calculated. $^{10}B\{^1H\}$ and $^{11}B\{^1H\}$ NOEs obtained upon broad-band presaturation of ^1H resonances were in all cases similar to the values predicted from dipolar contributions to ^{10}B and ^{11}B relaxation. Quadrupolar coupling constants of 5.2×10^5 Hz for ^{10}B and 2.5×10^5 Hz for ^{11}B in the BH_4^- anion were calculated. Quadrupolar contributions to boron relaxation in ion pair **1a** correlate with measured solution viscosity as a function of temperature under ion pairing conditions, but interionic $^1H\{^1H\}$ NOEs do not, showing a negative deviation from intensity expected as a result of viscosity. Increasing the size of the cation increases the deviation. It is concluded that magnitude and sign of interionic NOEs reflect the motion of the ion pair as a unit, and hence the effects of multiion aggregation, while the relaxation of the boron nucleus reflects more rapid motion independent of the ion pair. The correlation time of the interionic vector is used to predict a lower limit on the mean lifetime of a discrete ion binding mode.

Introduction

Ion pairing has been shown to have a profound influence on the physical and chemical behavior of ionic solutions and must be considered in any discussion of the behavior of ionic species in low dielectric solvents (and also for moderately concentrated solutions of ionic species in high dielectric solvents).[1] NMR techniques have often been applied to the problem of understanding ion pair structure and dynamics. NMR approaches include the analysis of field effects on chemical shift,[2] analysis of isotropic shifts in paramagnetic systems in terms of ion pair association and structural constraints,[3] dynamic NMR methods,[4] and line width analysis of quadrupolar nuclei.[5] Although most recent work has been directed toward understanding the reactivity of organometallic reagents,[6] some efforts have been made to understand the structure of closed-shell ion pairs as well. We have begun investigating the structure and dynamics of ion pairs formed in nonpolar solvents between quaternary ammonium ions and small hard anions. Of particular interest are those ion pairs which are implicated in phase-transfer reactions. This work is aimed at a better understanding of the mechanisms of phase-transfer reactions with an eye to designing catalysts for improved chemical or stereoselectivity. The tetraalkylammonium cations used in the present work are known to be catalytic for phase-transfer reactions between reagent anions and nonpolar substrates.[7,8] Tetrahydridoborate, BH_4^-, was chosen as the anionic probe for several reasons. First, BH_4^- is relevant to phase-transfer catalysis (PTC), being a commonly used phase-transfer reductant of ketones and aldehydes. Secondly, the ion contains three NMR-active nuclei, ^1H ($I = {}^1/_2$), ^{10}B ($I = 3$), and ^{11}B ($I = {}^3/_2$). As such, BH_4^- provides several different probes of the ion pair environment. Finally, the small size of BH_4^- (ionic radius = 1.9 Å)[9] makes it relatively nonperturbing toward the cationic structure. We recently reported the observation of significant interionic $^1H\{^1H\}$ and $^{11}B\{^1H\}$ nuclear Overhauser effects (NOEs) in a contact ion pair **1a** formed between the tetrahydridoborate anion, BH_4^-, and the tetrabutylammonium ion in $^2HCCl_3$

† Current address: Bruker Instruments, Billerica, MA.

⊛ Abstract published in *Advance ACS Abstracts,* October 15, 1993.

(1) (a) Szwarc, M. *Ions and Ion Pairs in Organic Reactions*, Wiley-Interscience: New York, 1972 and 1974; Vols. 1 and 2. (b) Hogen-Esch, T. E. *Adv. Phys. Org. Chem.* **1977**, *15*, 153–266. (c) Reichardt, C. *Solvents and Solvent Effects in Organic Chemistry*; VCH: Weinhiem, 1990.

(2) (a) Vos, H. W.; MacLean, C.; Velthorst, N. H. *J. Chem. Soc., Faraday Trans. 2* **1977**, *73*, 327. (b) Van der Kooij, J.; Velthorst, N. H.; MacLean, C. *Chem. Phys. Lett.* **1972**, 596. (c) Hogen-Esch, T. E.; Smid, J. *J. Am. Chem. Soc.* **1966**, *88*, 318. (d) Grutzner, J. B.; Lawlor, J. M.; Jackman, L. M. *J. Am. Chem. Soc.* **1972**, *94*, 2306.

(3) (a) Tsao, N.-Y.; Lim, Y.-Y. *Aust. J. Chem.* **1981**, *34*, 2321. (b) Chen, N.; Witton, P. J.; Holloway, C. E.; Walker, I. M. *J. Coord. Chem.* **1988**, *19*, 113. (c) Lim, Y.Y.; Drago, R. S. *J. Am. Chem. Soc.* **1972**, *94*, 84. (d) Quereshi, M. S.; Walker, I. M. *Inorg. Chem.* **1975**, *14*, 2187.

(4) (a) Honeychuck, R. V.; Hersh, W. H. *J. Am. Chem. Soc.* **1989**, *111*, 6056. (b) Kessler, H.; Feigel, M. *Acc. Chem. Res.* **1982**, *15*, 2. (c) Miller, J. M.; Clark, J. H. *J. Chem. Soc. Chem. Commun.* **1982**, 1318.

(5) Radley, K. *Mol. Cryst. Liq. Cryst., Lett. Sect.* **1989**, *6*, 203.

(6) (a) Bauer, W.; Muller, G.; Pi, R.; Schleyer, P. v. R. *Angew. Chem., Int. Ed. Engl.* **1986**, *25*, 1103. (b) Bauer, W.; Klusner, P. A. A.; Harder, S.; Kanters, J. A.; Duisenberg, A. J. M.; Brandsma, L.; Schleyer, P. v. R. *Organometallics* **1988**, *25*, 552. (c) Bauer, W.; Winchester, W. R.; Schleyer, P. v. R. *Organometallics* **1988**, *25*, 552. (d) Bauer, W.; Clark, T.; Schleyer, P. v. R. *J. Am. Chem. Soc.* **1987**, *109*, 970. (e) Bauer, W.; Feigel, M.; Muller, G.; Schleyer, P. v. R. *J. Am. Chem. Soc.* **1988**, *110*, 6033. (f) Hoffmann, D.; Bauer, W.; Schleyer, P. v. R. *J. Chem. Soc., Chem. Commun.* **1990**, 208.

(7) Weber, W. P.; Gokel, G. W. Phase Transfer Catalysis in Organic Synthesis; Springer-Verlag: New York, 1977.

(8) Dhemlow, E. V.; Dhemlow, S. S. *Phase Transfer Catalysis*; Verlag Chemie: Weinheim, 1980.

(9) Greenwood, N. N. In *Comprehensive Inorganic Chemistry:* Bailar, J. C. et al., Eds.; Pergamon Press: New York, 1971; Vol. 1, Chapter 11, p 746.

0002-7863/93/1515-11084$04.00/0

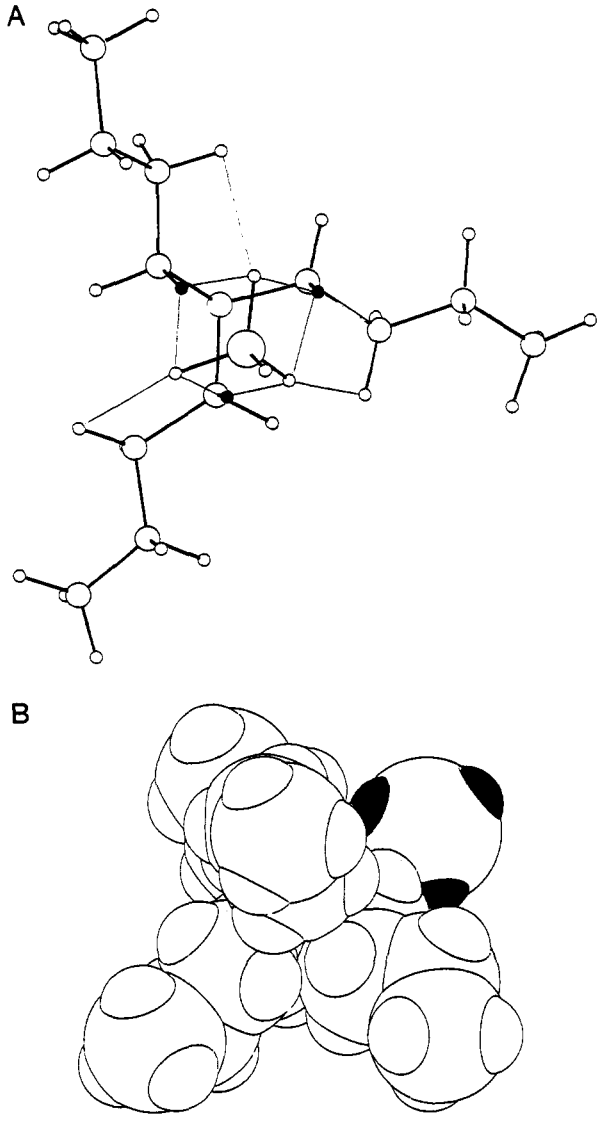

Figure 1. (A) Model for the time average solution structure of ion pair **1a**, based on observed interionic NOE intensities for a 0.2 M solution of ion pair **1a** in $^2HCCl_3$. A discrete ion binding mode is defined as occupation by BH_4^- of a trigonal-pyramidal site provided by three *n*-butyl chains of the cation as shown. van der Waals contacts between the BH_4^- hydrogens and the cation are shown by the thin lines; the hexagonal pattern connects each BH_4^- proton with two 1-CH_2 protons, and the three radial lines connect each BH_4^- proton with one 2-CH_2 proton. The fourth *n*-butyl side chain is not shown for clarity. (B) Side-on view of the same model showing the nonequivalence of the alkyl groups of the cation. The BH_4^- protons are shown in black. As only one set of *n*-butyl resonances are observed, exchange between discrete binding modes is fast on the ^1H chemical shift time scale.

solution.[10] A time average solution structure for ion pair **1a** was proposed which rationalized the observed effects (Figure 1).

It may be inferred from a large body of data that ion pairs show preferences for certain relative configurations of cation and anion, and these preferences are reflected in experimental observables such as dipole moments, optical and magnetic resonance spectroscopic properties.[1-6,11] However, until recently, it was not possible to obtain direct structural information concerning the time average structures of ion pairs. Now, using interionic NOEs, we are able to obtain direct information regarding the relative configurations of cation and anion in closed-shell ion pairs of type **1**. The use of the NOE for the structural characterization of monomeric and polymeric solution species is well-established, and the limitations of the methodology have been discussed in detail.[12] Intermolecular NOEs may also be used to characterize solution complexes and noncovalent aggregates, but their interpretation is somewhat more complicated, and it is appropriate to consider how such data may be legitimately interpreted.

The NOE is a manifestation of cross-relaxation processes resulting from dipole–dipole (dd) interactions between two nuclei and provides information concerning the proximity of the two nuclei. The effect is observed as a change in signal intensity for the NMR signal of one spin upon perturbing the population of the second spin (by saturation or inversion) and exhibits a r^{-6} dependence on the distance between the two spins. Practically, this distance dependence prevents the observation of NOEs between nuclei which are greater than ca. 5 Å apart. In cases where chemical exchange causes the distance r to vary, the observed NOE is dependent on $\langle r^{-6} \rangle$, the weighted time average of the r^{-6} in the ensemble of populated structures.[12] Steady-state is reached in the NOE experiment on a time scale of the order of T_1 for the observed spin, and any chemical process which comes to equilibrium much faster than T_1 will result in the equilibrated structures each contributing to the NOE in proportion to the fraction of time spent in that structure and the inverse sixth power of the distance between the spins from which the NOE originates in that structure. Thus, no information is available from a given NOE concerning populated structures which do not bring the two nuclei responsible for that NOE into proximity, no matter what the relative populations of those structures might be. Also, a given structure will not contribute in equal proportion to all of observed NOEs, and, as a result, no one structure may fit all of the data. Finally, although precise internuclear distance information may be calculated from the intensity of the NOE in nonexchanging systems, too many assumptions concerning contributing structures and their populations are required for such calculations to be made reliably in exchanging systems. Still, the NOE in exchanging systems provides reliable information on average *relative* internuclear distances, and if interpreted cautiously, is a valuable tool for structural characterization of solution complexes.[13]

Ion pairs are fluxional species, and characterization of dynamics is also important to an understanding of the phenomenon. Far infrared vibrational modes (ca. 100 cm^{-1}) have been observed spectroscopically for ion pairs similar to **1a** in nonpolar solvents and have been assigned to oscillations in the interionic distance.[14] Exchange between discrete binding modes (that is, BH_4^- occupation of one trigonal-pyramidal site created by three alkyl side chains of the cation) is fast on the ^1H chemical shift time scale for ion pairs of type **1**. Only one set of alkyl resonances are observed for the cation, although a discrete ion-binding mode would have two distinct magnetic environments for the cationic alkyl protons, with one alkyl group not in contact and three in contact with the anion (see Figure 1). Considerable evidence also suggests that ion pairs of type **1** can aggregate to form higher order multipoles, which further complicates the problem of analyzing the dynamics of such systems.[15-17]

The NOE and nuclear relaxation are powerful tools for characterization of dynamics. Nuclear relaxation depends on fluctuations in the local electromagnetic environment to stimulate transitions. For dipolar nuclei ($I = {}^1/_2$), relaxation is usually

(10) Pochapsky, T. C.; Stone, P. M. *J. Am. Chem. Soc.* **1990**, *112*, 6714–6715.
(11) Begum, M. K., Grunwald, E. J. *J. Am. Chem. Soc.* **1990**, *112*, 5104–5110.
(12) Neuhaus, D.; Williamson, D. *The Nuclear Overhauser Effect in Structural and Conformational Analysis*; VCH Publishers: New York, 1989.
(13) Pirkle, W. H.; Pochapsky, T. C. *J. Am. Chem. Soc.* **1987**, *109*, 5975–5982.
(14) Evans, J. C.; Lo, G. Y-S. *J. Phys. Chem.* **1965**, *69*, 3223.
(15) Copenhafer, D. T.; Kraus, C. A. *J. Am. Chem. Soc.* **1951**, *73*, 4557.
(16) Shen, Y.; Liu, X.; Ma, X.; He, X. *J. Jilin Univ.* **1987**, *3*, 113–115.
(17) Stone, P. M.; Pochapsky, T. C.; Callegari, E. *J. Chem. Soc., Chem. Commun.* **1992**, 178–179.

Table I. Steady-State Interionic $^1H\{^1H\}$ NOEs in Ion Pair **1a** as a Function of Solvent[e]

saturated	C^2HCl_3[a]	D_2O[b]	DMSO-d_6[c]	benzene-d_6[a,d]
1-CH_2	0.180	~0.01	0.073	0.071
2-CH_2	0.081	<0.01	0.030	0.029
3-CH_2	0.035	<0.01	<0.01	
4-CH_3	0.010	<0.01	<0.01	

[a] 0.2 M, 298 K. [b] 0.2 M, 278 K. [c] 0.2 M, 295 K. [d] Overlap of the BH_4^- protons and the 3-CH_2 and 4-CH_3 resonances in [$^2H_6$]benzene prevented the performance of these experiments. [e] All measurements were made at 300 MHz.

mediated at least in part by time-dependent dipolar couplings to other nuclei or electrons. For nuclei with $I > 1/2$, quadrupolar pathways typically dominate relaxation. Quadrupolar relaxation depends on fluctuations in the local electric field gradient (EFG). The efficiency of dipolar and quadrupolar processes therefore depend on the spectral density, $J(\omega)$, of fluctuations in the local magnetic field and EFGs, respectively, at the transition frequency ω.[18] For this reason, relaxation provides a probe of dynamics. In the present work, we are concerned with motions which determine relaxation of ^{10}B and ^{11}B in the BH_4^- anion as well as those which affect the sign and intensity of interionic NOEs observed upon selective saturation of cationic proton resonances.[17]

Results and Discussion

Interionic NOEs as a Function of Solvent in Ion Pair 1a. Our preliminary communication concerning the observation of interionic $^1H\{^1H\}$ and $^1H\{^{11}B\}$ NOEs in ion pair **1a** described specific interionic NOEs observed for a 0.2 M solution of ion pair **1a** in $^2HCCl_3$. The observed effects (listed in Table I) were rationalized by the model for the time average solution structure of ion pair **1a** shown in Figure 1.[10] In this model, each of three BH_4^- hydrogens are placed in van der Waals contact with two 1-CH_2 and one 2-CH_2 protons in the trigonal-pyramidal site provided by the cation. All three alkyl side chains are in staggered conformation, and a C_3 symmetry axis lies along the N–B internuclear vector. Using CPK models, a N–B distance of 3 Å is estimated, which is reasonable in light of the metal–boron bond distances in alkali tetrahydridoborates, which range from 2.5 to 3.7 Å.[9] If a simple "on–off" description of the ion pair is assumed (that is, only one structure is giving rise to NOEs), the ca. 2:1 ratio between the magnitude of NOEs observed at the BH_4^- ^1H resonances upon selective saturation of the 1-CH_2 and 2-CH_2 ^1H resonances (the $BH_4^-\{1\text{-}CH_2\}$ and $BH_4^-\{2\text{-}CH_2\}$ NOEs, respectively)[19] may be rationalized in terms of the van der Waals contacts between cation and anion described above (see Figure 2). The model is supported by the observation of a 2.1% positive $^{11}BH_4^-\{1\text{-}CH_2\}$ NOE, while a negative (–0.8%) $^{11}BH_4^-\{2\text{-}CH_2\}$ NOE is observed. In small molecules with short correlation times, negative NOEs are the result of indirect effects transmitted to the observed nucleus from the perturbed nucleus via a third spin, which normally experiences a significant direct (positive) NOE in the same experiment. The large NOEs at the BH_4^- protons resulting from saturation of the 1-CH_2 and 2-CH_2 resonances should produce a significant indirect effect at ^{11}B. Apparently, the direct NOE predominates when the 1-CH_2 resonance is saturated, while indirect effects predominate from the 2-CH_2 protons. Both observations are predicted by the model in Figures 1 and 2.

The magnitude and relative intensities of the interionic NOEs observed suggest that contact ion pairs predominate for **1a** in $^2HCCl_3$. It was of interest to see whether interionic NOEs might be used to provide information concerning the type and extent of ion pairing in other solvents. The results of these experiments are also summarized in Table I. It was noted that reduced but still significant interionic $^1H\{^1H\}$ NOEs are observed both in [$^2H_6$]benzene and [$^2H_6$]dimethyl sulfoxide, with $BH_4^-\{1\text{-}CH_2\}/BH_4^-\{2\text{-}CH_2\}$ NOE ratios similar to that observed in $^2HCCl_3$. The decrease in observed NOEs may indicate that ion pair **1a** is somewhat more dissociated in these solvents than in $^2HCCl_3$, although differences in solvent viscosity or aggregation may account for the loss of NOE intensity (vide infra). Also interesting is that in [$^2H_6$]benzene, the BH_4^- protons show a significant (0.85 ppm) *downfield* shift relative to their positions in other solvents; this is counter to the upfield shift usually observed upon transfer of a solute from $^2HCCl_3$ to [$^2H_6$]benzene.[20] The net effect of shielding anisotropy for small molecules in benzene is typically an upfield shift; in the absence of specific interactions, random interactions place the small molecule most of the time in the shielding region of the aromatic ring. In the present case, however, it is likely that the size of the benzene molecule prevents it from approaching the anion in the binding site face-on but must approach the binding site edge-on to pack efficiently and solvate the ion pair.

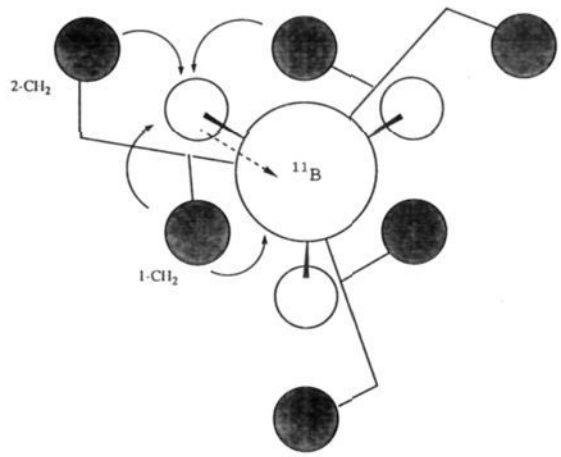

Figure 2. Diagram rationalizing observed NOE intensities in ion pair **1a** using the model proposed in Figure 1. The approximately 2:1 ratio of the $BH_4^-\{1\text{-}CH_2\}/BH_4^-\{2\text{-}CH_2\}$ NOE is predicted by the ratio of van der Waals contacts to each BH_4^- hydrogen (solid arrows), as is the predominance of the direct (solid arrow) over the indirect (dotted arrow) $^{11}BH_4^-\{1\text{-}CH_2\}$ NOE, while only indirect effects are seen for the $^{11}BH_4^-\{2\text{-}CH_2\}$ NOE.

It is clear that ion pair **1a** is almost completely dissociated (or at least solvent-separated) in ^2H_2O. Only small, nonspecific interionic NOEs are observed at temperatures above 278 K for this system. At 278 K, the $BH_4^-\{1\text{-}CH_2\}$ NOE is somewhat larger than those observed upon saturation of the other alkyl resonances, but the difference is too small to be interpreted with confidence.

Interionic NOEs as a Function of Temperature in Ion Pairs 1a, 1b, and 1c: Evidence for Multiion Aggregation. We have previously reported that observed interionic $BH_4^-\{1\text{-}CH_2\}$ NOEs exhibit an unusual temperature dependence in that large negative intensity changes occur with decreasing temperature in $^2HCCl_3$.[17] For ion pair **1a**, this results in a decrease in the $BH_4^-\{1\text{-}CH_2\}$ NOE intensity from 14.7% at 298 K to zero at 223 K. However, a rotating-frame NOE experiment (ROESY) performed at 223 K confirms that ion pair **1a** is still strongly associated, and the lack of a steady-state NOE at 223 K is not due to dissociation of the ion pair.[17] For ion pairs involving larger cations (tetra-*i*-amylammonium tetrahydridoborate **1b** or tetraoctylammonium tetrahydridoborate **1c**) the negative intensity change is enhanced;

(18) Abragam, A. *Principles of Nuclear Magnetism*; Oxford University Press: London, 1961.

(19) In the format used here for describing NOE experiments, the boldface nucleus within the bracket represents the resonance which is saturated, while the NOE is observed to the resonance corresponding to the boldface nucleus outside the brackets. Hence, $^{11}BH_4^-\{1\text{-}CH_2\}$ represents the observation of NOE at ^{11}B while saturating the 1-methylene protons.

(20) Lambert, J. B.; Shurvell, H. F.; Verbit, L.; Cooks, R. G.; Stout, G. H. *Organic Structural Analysis*; Macmillan Publishing Co.: New York, 1976; pp 44–45.

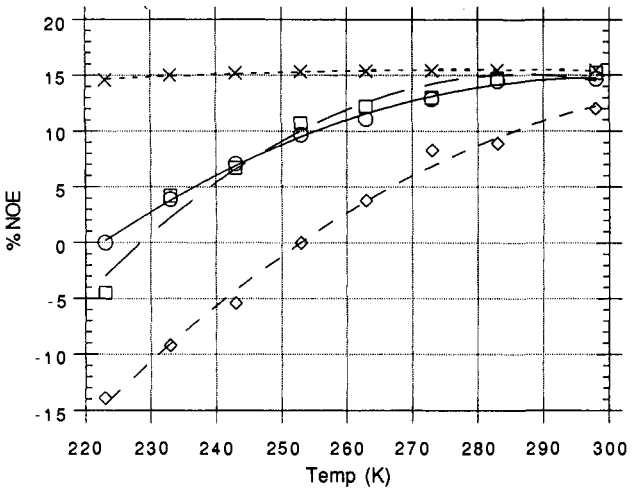

Figure 3. Percent $BH_4^-\{1\text{-}CH_2\}$ NOE vs temperature for 0.2 M solutions of ion pairs **1a** (○), **1b** (□), and **1c** (◇) in $^2HCCl_3$. The curve defined by (×) is the percent $BH_4^-\{1\text{-}CH_2\}$ NOE predicted for ion pair **1a** from experimentally-determined viscosities using eqs 1 and 3, assuming a maximum NOE enhancement at the extreme narrowing limit of 15.5%, a radius for the ion pair of 4.6 Å and a transition frequency of 1.884×10^9 rad s^{-1}.

the same experiment for ion pair **1b** results in an intensity decrease for the $BH_4^-\{1\text{-}CH_2\}$ NOE from 15.2% at 298 K to –4.5% at 223 K, while the tetraoctylammonium **1c** species goes from 12% $BH_4^-\{1\text{-}CH_2\}$ NOE at 298 K to –13.9% at 223 K (see Figure 3).

The sign and magnitude of the homonuclear NOE is dependent on the Larmor frequency ω_c of the observed nucleus (in angular frequency units) and on the rotational correlation time τ of the observed species.[21] The maximum fractional enhancement f_{max} (as defined in the Experimental Section, *vide infra*) is given by eq 1.

$$f_{max} = (5 + \omega_c^2\tau^2 - 4\omega_c^4\tau^4)(10 + 23\omega_c^2\tau^2 + 4\omega_c^4\tau^4)^{-1} \quad (1)$$

At short correlation times (small molecules, nonviscous solvents, $\omega_c^2\tau^2 \ll 1.2$), eq 1 predicts an $f_{max} = 0.5$. At long correlation times (macromolecules, viscous solvents, $\omega_c^2\tau^2 \gg 1.2$) the expression predicts an $f_{max} = -1$. At intermediate correlation times ($\omega_c^2\tau^2 \sim 1.2$) the NOE approaches zero. It is assumed that the observed interionic NOEs at 298 K for ion pairs **1a** and **1b** represents the maximum positive value observable at the extreme narrowing limit. As the slopes of the curves for **1a** and **1b** in Figure 3 flatten out at higher temperatures, this does not seem an unreasonable assumption. If the expected correlation time of the species being observed is determined, f_{max} may be calculated using eq 1. This calculated value of f_{max} is then used to scale the maximum observable interionic NOE as a function of correlation time, giving the fourth (theoretical) curve shown in Figure 3.

In order to calculate correlation times, experimental values of the solution viscosity are required. Measured viscosity of a 0.2 M solution of **1a** in $CHCl_3$ as a function of temperature is shown in Table V. A number of semiempirical and empirical relationships between the rotational correlation time and macroscopic solution properties, that is, viscosity and temperature have been derived. The most commonly used is the Stokes–Einstein eq 2

$$\tau = 4\pi\eta r^3/3kT \quad (2)$$

where η is the viscosity of the solution, r is the radius of the reorienting species, k is Boltzmann's constant, and T is the absolute temperature. Calculations of expected values for f_{max} in ref 17 were made using a value of τ determined with eq 2.[17] However, eq 2 tends to predict a correlation time roughly an order of magnitude larger than those observed experimentally, except for small polar species.[22,23] In the present work, the modified relationship of Gierer and Wirtz,[24] eq 3, is used to calculate the expected correlation time τ for a simple ion pair:

$$\tau = \eta(V_{solute})(r_{solute})/6kT(r_{solvent}) \quad (3)$$

where η is the solution viscosity, r_{solute} is the radius of the solute species, $r_{solvent}$ the radius of the solvent molecule (taken as 2.75 Å, based on a C–Cl bond length of 1.76 Å and a covalent radius of 0.99 Å for Cl),[25] and V_{solute} is the hard-sphere volume of the ion pair, calculated using a value of 4.6 Å for r_{solute}, as estimated from CPK models. If f_{max} is calculated using rotational correlation times derived with eq 3, a significantly smaller deviation from the extreme narrowing condition as a function of temperature is predicted than what is calculated using the Stokes–Einstein eq 2.[17]

One possible explanation for the observed deviations from the sign and intensity of f_{max} predicted by eq 1 and 3 for the $BH_4^-\{1\text{-}CH_2\}$ NOE observed in ion pairs **1a**, **1b**, and **1c** is the increased tendency toward multiion aggregate formation with decreasing temperature.[17] Kraus noted significant aggregation in solutions of tetrabutylammonium halides in benzene using freezing point depression methods.[15] Shen and co-workers detected significant amounts of aggregation by vapor pressure methods for tetraalkylammonium bromides in benzene and chloroform.[16] We observed only a very slight freezing point depression (ΔT_f = –0.03 K) for a 0.2 molal solution of **1a** in $CHCl_3$. This may be compared to a ΔT_f = –0.66 K for a 0.2 molal benzene solution in $CHCl_3$ measured under the same conditions. There is some loss of solubility of **1a** at low temperatures, so an accurate aggregation number could not be obtained from these measurements. However, the small freezing point depressions observed are consistent with significant aggregation.

Table II. ^{10}B Relaxation Rate Constants, T_1^{-1}, and Fractional $^{10}B\{^1H\}$ NOE Enhancements, f_s, for Solutions of **1a** and $NaBH_4$ **2** Measured at 32.24 MHz[a]

salt/solvent	$T_1^{-1}{}_{obs}$	T_1^{-1}(dd)	T_1^{-1}(q)	f_s(calc)	f_s(obs)
0.2 M **1a**/C^2HCl_3[c]	0.191 (0.010)	0.009	0.182	0.21	0.15
0.2 M **1a**/^2H_2O[c]	0.106 (0.010)	0.003	0.103	0.13	0.12
0.2 M **1a**/$[^2H_6]$DMSO[c]	0.063 (0.003)	0.006	0.057	0.42	0.23
0.1 M **2**/^2H_2O[d]	0.049 (0.002)	0.003	0.046	0.28	0.21
0.1 M **2**/$[^2H_6]$DMSO[e]	0.103 (0.006)	0.003	0.100	0.15	0.11

[a] Experimental uncertainties for $T_1^{-1}{}_{obs}$ are shown in parentheses. All T_1^{-1} values are in units of s^{-1}. Values for f_s(calc) are obtained from eq 4 and f_s(obs) are calculated as described in the Experimental Section. [b] Temperatures at which measurements were made are as follows: 25.0 °C, [d] 2.0 °C, [e] 18.4 °C.

Dipolar and Quadrupolar Contributions to ^{10}B and ^{11}B T_1s. The motion of the BH_4^- anion is correlated with cation motion as a result of being held in a discrete ion binding site, as shown in Figure 1. This is clearly indicated by the temperature dependence of the interionic $^1H\{^1H\}$ NOE. However, the anion should, within the confines of the binding site, have significant freedom to reorient; the coulombic forces responsible for ion pairing are not expected to be highly directional. Reorientation of the anion perturbs the interaction of the boron nuclear quadrupole with local EFGs, causing boron nuclear relaxation. Boron relaxation rates then should reflect the dynamics of this reorientation.

Boron T_1 relaxation rates and $^{10}B\{^1H\}$ and $^{11}B\{^1H\}$ NOEs for the BH_4^- anion for a number of different solvents and counterions are shown in Tables II and III. As noted above, relaxation of

(21) Noggle, J. H.; Schirmer, R. E. *The Nuclear Overhauser Effect: Chemical Applications*; Academic Press: New York, 1971.

(22) Marks, T. J.; Shimp, L. A. *J. Am. Chem. Soc.* **1972**, *94*, 1542–1550.

(23) Woessner, D. E.; Snowden, B. S., Jr.; Strom, T. E. *Mol. Phys.* **1968**, *7*, 515.

(24) Gierer, A.; Wirtz, K. *Z. Naturforsch. A.* **1953**, *8*, 532.

(25) *Tables of Interatomic Distances and Configuration in Molecules and Ions*; Sutton, L., Ed.; Spec. Publ. No. 11 and 18, The Chemical Society: London, 1958 and 1965.

Table III. ^{11}B Relaxation Rate Constants, T_1^{-1}, and Fractional $^{11}B\{^1H\}$ NOE Enhancements, f_s, for Solutions of **1a** and **2** Measured at 96.25 MHz[a]

salt/solvent	$T_1^{-1}{}_{obs}$	T_1^{-1}(dd)	T_1^{-1}(q)	f_s(calc)	f_s(obs)
0.2 M **1a**/C^2HCl_3[c]	0.355 (0.004)	0.074	0.280	0.33	0.31
0.2 M **1a**/^2H_2O[c]	0.16 (0.02)	0.022	0.159	0.19	0.21
0.2 M **1a**/$[^2H_6]$DMSO[c]	0.137 (0.001)	0.048	0.088	0.55	0.36
0.1 M **2**/^2H_2O[d]	0.096 (0.003)	0.025	0.071	0.40	0.39
0.1 M **2**/$[^2H_6]$DMSO[c]	0.182 (0.001)	0.029	0.153	0.24	0.14

[a] Experimental uncertainties for $T_1^{-1}{}_{obs}$ are shown in parentheses. All T_1^{-1} values are in units of s^{-1}. Values for f_s(calc) are obtained from eq 4, and f_s(obs) are calculated as described in the Experimental Section. [b] Temperatures at which measurements were made are as follows: 25.0 °C, [d]20.0 °C, [e]18.4 °C.

Table IV. Temperature Dependence of Observed ^{10}B and ^{11}B T_1 Values and Correlation Times τ_c for BH_4^- Calculated from eq 3 Using Experimental Viscosities (Table V) and a Radius of 1.9 Å for the BH_4^- Ion for a Solution of 0.2 M **1a** in $^2HCCl_3$[a]

temp (K)	^{10}B T_1 (s)	^{11}B T_1 (s)	τ_c (s)
298	5.1 (0.1)	2.90 (0.05)	1.05×10^{-12}
273	3.7 (0.3)	2.20 (0.03)	1.63×10^{-12}
248	2.4 (0.4)	1.40 (0.02)	2.55×10^{-12}
223	1.3 (0.3)	0.86 (0.01)	5.25×10^{-12}

[a] Relaxation measurements were made at 32.24 and 96.25 MHz for ^{10}B and ^{11}B, respectively. Experimental uncertainties for T_1 values are shown in parentheses.

nuclei with $I > {}^1/_2$ is typically dominated by quadrupolar pathways. However, ^{10}B (I = 3) and ^{11}B ($I = {}^3/_2$) relaxation in BH_4^- is not completely dominated by quadrupolar effects because the boron nucleus is at a site of high symmetry (T_d), and, as such, the electric field gradient (EFG) at the nucleus averages to zero over time. In all of the present cases, $^{10}B\{^1H\}$ and $^{11}B\{^1H\}$ NOEs are observable, providing evidence that dipole–dipole (dd) mechanisms are significant in the relaxation of the boron nucleus in BH_4^-.

The maximum observable NOE enhancement possible to a nucleus S, f_S, upon saturation of nucleus I is given by eq 4

$$f_S = 0.5\gamma_I(\gamma_s)^{-1}(1/T_1{}^S{}_{dd})(1/T_1{}^S{}_{dd} + 1/T_1{}^S{}_{other})^{-1} \quad (4)$$

where γ_I and γ_S are the gyromagnetic ratios of the irradiated and observed nuclei, respectively, $1/T_1{}^S{}_{dd}$ is the contribution to spin–lattice relaxation of spin S from dd interaction with spin I, and $1/T_1{}^S{}_{other}$ represents contributions from all other pathways.[26] Equation 4 yields a $f_S = 1.56$ for ^{11}B and $f_S = 4.65$ for ^{10}B, as the NOE expected to either nucleus if proton-mediated dd pathways are the only significant contributor to ^{10}B and ^{11}B relaxation. Much smaller steady-state enhancements are observed upon composite-pulse presaturation of the ^1H resonances in the cases described here; ^{10}B shows values for f_S ranging from 0.12 to 0.23 and ^{11}B values ranging from 0.21 to 0.39.

Other potential contributors to relaxation besides dd and quadrupolar (q) processes include chemical shift anisotropy (csa) and spin-rotation coupling (sr). Although csa is unlikely to be important for relaxation in a symmetric ion such as BH_4^-, it was considered that ion pairing might cause sufficient anisotropy to permit appreciable csa. However, ^{11}B T_1 values obtained for 0.2 M **1** in $^2HCCl_3$ at 96.25 and at 160.42 MHz were the same within experimental error. As ^{11}B is the nucleus which is more susceptible to csa relaxation, this pathway is likely to be unimportant for either ^{10}B or ^{11}B. Finally, sr relaxation, which becomes more efficient as temperature increases, does not seem to be a significant contributor to boron T_1 relaxation, based on the temperature dependence of boron T_{1obs} for **1a**, which decreases with decreasing temperature (see Table V). Even if sr relaxation is only one of several competing mechanisms for longitudinal relaxation, a minimum in a plot of $T_1^{-1}{}_{obs}$ versus temperature is expected, which is also not observed.[27] Eliminating all but dd and q contributions to boron relaxation in the extreme narrowing limit, the relative contributions of each mechanism to T_{1obs} may be calculated based on the following considerations.

Table V. Viscosity as a Function of Temperature for a 0.2 M Solution of **1a** in $CHCl_3$

temp (K)	viscosity (centipoise)	temp (K)	viscosity (centipoise)
232	1.919	282	0.829
245	1.403	295	0.675
263	1.063		

Ignoring cross-correlation, the observed relaxation of both boron nuclei is described by eqs 5 and 6

$$1/T_{1obs}(^{10}B) = 1/T_{1dd}(^{10}B) + 1/T_{1q}(^{10}B) \quad (5)$$

$$1/T_{1obs}(^{11}B) = 1/T_{1dd}(^{11}B) + 1/T_{1q}(^{11}B) \quad (6)$$

$$1/T_{1qI} = 3\pi^2(2I + 3)(1 + \eta^2/3)[10I^2(2I - 1)]^{-1}\chi_I{}^2\tau_c \quad (7)$$

$$1/T_{1ddI} = {}^4/_3\gamma_I{}^2\gamma_S{}^2h(1/2\pi)S(S + 1)\tau_c\sum^{i} r_{ISi}{}^{-6} \quad (8)$$

Equations 7 and 8 describe the quadrupolar and dipolar contributions, respectively, to T_{1obs} of spin I at the extreme narrowing limit. However, eq 7 requires knowledge of the quadrupolar coupling constant, χ, the rotational correlation time, τ_c, and the molecular asymmetry parameter η (where I is the spin of the quadrupolar species I) for solution.[28,29] τ_c is also required for the solution of eq 8, in which S is the spin of nucleus S with which spin I is coupled, h is Planck's constant, the γ_i are the gyromagnetic ratios of I and S, and r_{ISi} is the internuclear distances for I and the ith spin S.

The quadrupolar coupling, χ, is difficult to obtain directly in solution. However, it can be seen from eq 9

$$\chi = eQ(eq_{zz})/h \quad (9)$$

where e is the elementary charge, Q is the nuclear quadrupole moment, h is Planck's constant and eq_{zz} is the EFG at the nucleus, that the quadrupolar coupling constants for the two isotopes of boron in identical environments will be related by the ratios of their respective nuclear quadrupole moments, which are known.[30] As such, the ratio of the χ_i of ^{10}B and ^{11}B in a given environment may be calculated. By the same logic, expected ratios (^{10}B)-$T_{1dd}/(^{11}B)T_{1dd}$ and $(^{10}B)T_{1q}/(^{11}B)T_{1q}$ may also be calculated based on the cancellation of internuclear distances, correlation times, and EFGs from eqs 7 and 8:

$$T_{1dd}(^{11}B)/T_{1dd}(^{10}B) = {}^{10B}\gamma^2/{}^{11B}\gamma^2 = 0.112 \quad (10)$$

$$T_{1q}(^{11}B)/T_{1q}(^{10}B) = 0.15[{}^{10B}\chi^2/{}^{11B}\chi^2] = 0.651 \quad (11)$$

Now, eqs 5 and 6 may be solved for the T_{1q} and T_{1dd} of both nuclei from the values of T_{1obs}. Similar approaches have been used to determine that quadrupolar relaxation pathways predominate for ^{10}B and ^{11}B in aqueous solutions of boric acid[31] and to estimate quadrupolar couplings in symmetric transition metal tetrahydridoborates and in BH_3NH_3.[22,32] The intensities of observed $^{10}B\{^1H\}$ and $^{11}B\{^1H\}$ NOEs provide an independent test

(26) Harris, R. K. *Nuclear Magnetic Resonance Spectroscopy*; Pitman Books, Ltd.: London, 1983; p 108.

(27) Sharp, R. R. *J. Chem. Phys.* **1972**, *57*, 5321–5330.

(28) Bloembergen, N. *Nuclear Magnetic Relaxation*; Benjamin: New York, 1961; p 118ff.

(29) Hertz, H. G. *Ber. Bunsenges. Phys. Chem.* **1973**, *77*, 531.

(30) Values of 2.876×10^7 rad/T s (^{10}B) and 8.5843×10^7 rad/T s (^{11}B) for the γi and 8.5×10^{26} m^2 (^{10}B) and 4.1×10^{26} m^2 (^{11}B) for the nuclear quadrupole moments were obtained: *Handbook of Chemistry and Physics*. 55th ed.; CRC Press: 1974–75; pp B248–332.

(31) Balz, R.; Brandle, U.; Kammerer, E.; Kohnlein, D.; Lutz, O.; Nolle, A.; Schafitel, R.; Veil, E. *Z. Naturforsch.* **1986**, *41a*, 737–742.

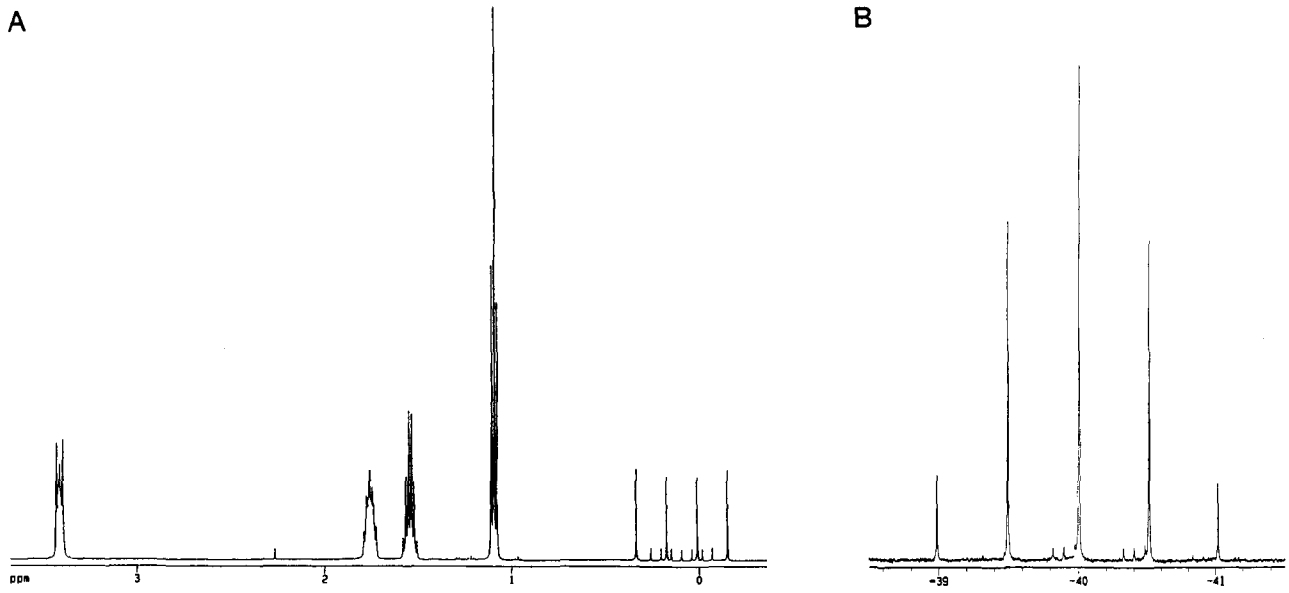

Figure 4. (A) 500-MHz ^1H NMR spectrum of **1a** (0.2 M in $^2HCCl_3$). Chemical shifts are referenced to tetramethylsilane. The $^{11}BH_4^-$ quartet and $^{10}BH_4^-$ septet are centered at 0.10 ppm. Cationic resonances are assigned as follows: 1-CH_2, 3.40 ppm; 2-CH_2, 1.75 ppm; 3-CH_2, 1.55; 4-CH_3, 1.09 ppm. (B) 160.42-MHz ^{11}B NMR spectrum of **1a** (0.2 M in $^2HCCl_3$). The chemical shift, in ppm, is referenced to external $BF_3{\cdot}Et_2O$ in $^2HCCl_3$. Note the low intensity quartet of triplets centered at −41.1 ppm resulting from the presence of deuterium-substituted BH_4^-.

of the accuracy of the calculation. Substituting the calculated dipolar contributions to boron relaxation into eq 4, the expected f_{max} for $^{10}B\{^1H\}$ and $^{11}B\{^1H\}$ NOEs may be calculated (see Tables II and III). Reasonable agreement between calculated and observed f_{max} values is observed in the cases discussed here. Since eqs 7 and 8 are valid at the extreme narrowing limit, the agreement between experimentally determined and predicted values for T_{1dd} and T_{1q} for both ^{10}B and ^{11}B indicate that no stochastic processes are occurring with frequencies in the range between the transition frequencies of the two nuclei (10^8–10^9 radians/s).

Temperature and Viscosity Dependence of ^{10}B and ^{11}B T_{1q}s in Ion Pair 1a and Estimate of ^{10}B and ^{11}B Quadrupolar Coupling in BH_4^-. For analysis of ^{10}B and ^{11}B relaxation, the relevant spectral densities are those which describe random fluctuations in the EFG at the boron nucleus. Although the origin of these fluctuations is unclear (vide infra), the data in Tables II and III indicate that the extent of ion pairing seems to have little or no effect on boron relaxation. Differences in ^{10}B and ^{11}B relaxation upon switching solvents and/or cations are subtle and do not appear to correlate with the extent of ion pairing. Even under conditions of extensive ion pairing (ion pair **1a** in $^2HCCl_3$), a temperature study of ^{10}B and ^{11}B relaxation shows that the quadrupolar contribution to relaxation, T_{1q}, correlates as expected with macroscopic viscosity and temperature based on eqs 3 and 7 (see Figure 5). These observations, along with the lack of csa effects on ^{10}B and ^{11}B relaxation in ion pair 1a, imply that discrete ion binding modes are not distinguished by the boron nuclei. We interpret this to indicate that any distortions in the electronic environment of the boron nucleus due to ion pairing is averaged over all possible relative orientations of the cation and anion by rapid reorientation of the BH_4^- anion. Furthermore, any aggregation which occurs must be sufficiently "loose" to allow significant contact between the anion and solvent; anions are apparently not sequestered in a "box" of cations for a significant fraction of the time.

Using measured solution viscosities to estimate rotational correlation times τ_a for the BH_4^- anion (r = 1.9 Å) from eq 3 and calculated values for T_{1q} as a function of temperature from Table IV, values of χ for ^{10}B and ^{11}B may be estimated with eq 7. For ^{10}B, χ averages 5.23×10^5 s^{-1}, while for ^{11}B, the average value

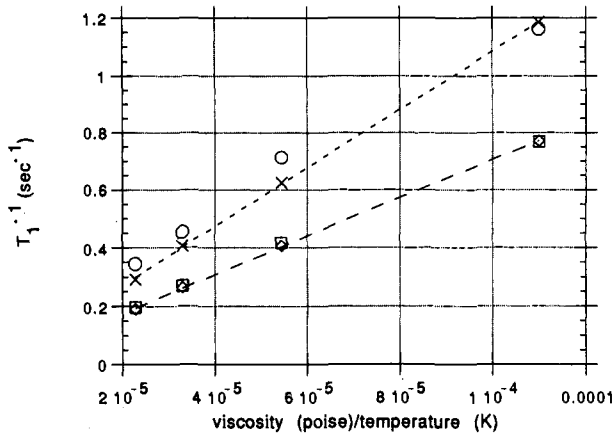

Figure 5. Plot of (^{10}B) $1/T_{1obs}$ (□), (^{10}B) $1/T_{1q}$ (◇), (^{11}B) T_{1obs} (○) and (^{11}B) T_{1q} (×) versus solution viscosity (obtained from data shown in Table V) divided by temperature (cp/K) for 0.2 M solution of **1a** in $^2HCCl_3$. Values for quadrupolar contributions to T_{1obs} were calculated as described in the text.

for χ is 2.51×10^5 s^{-1}. Both values are less than that estimated by Marks and Shimp for boron in multidentate metal–BH_4^- complexes by almost an order of magnitude. This is consistent with the ionic nature of the BH_4^- in **1a**, as opposed to the dative covalent bonding between metal and hydride thought to exist in the multidentate transition metal complexes.[22]

Types of Motion within Ion Pair 1. Although available evidence favors the proposal that ion pairs can have well-defined time-average structures, they differ from covalent species in that the electrostatic interactions which hold ion pairs together are for the most part nondirectional. Many degrees of motional freedom exist for ions within the pair and may contribute in varying amounts to observed relaxation behavior. Furthermore, evidence presented here and by other workers indicate that ion pairs are capable of forming higher order aggregates, although in most cases these aggregates are not discretely observable by NMR methods due to fast exchange. Hence, the observed spectroscopic behavior of a given ion pair reflects a weighted time average of the spectroscopic properties of the individual contributing structures. The observation of only a single set of ^1H resonances for the butyl groups of ion pair **1** indicate that that BH_4^- anion

(32) Penner, G. H.; Daleman, S. I.; Custodio. A. R. *Can. J. Chem.* **1992**, *70*, 2420–2423.

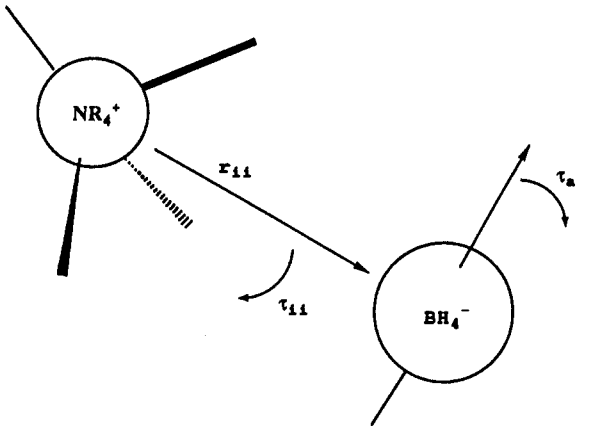

Figure 6. Independent motions in ion pair **1**. Motion of the interionic vector r_{ii} is described by τ_{ii} and is reflected in the interionic NOE. Tumbling of the BH_4^- anion (τ_a) is reflected in the relaxation behavior of the boron nucleus.

is exchanging between discreet cationic binding modes rapidly on the ^1H chemical shift time scale ($\gg 10^2$ s^{-1}). However, the lack of large ion-pairing effects on boron relaxation indicates motion of the BH_4^- anion is rapid enough to average instantaneous distortions in the electronic structure of the anion due to pairing over all orientations. A satisfactory theoretical description for the distortions which are responsible for nonzero quadrupolar coupling in symmetric molecules is still lacking, as recently reviewed by Kowalewski.[33] It has been shown that the EFG does not vanish at the center of symmetry for some vibrationally excited states of symmetric molecules,[34,35] and it has been proposed that these vibrationally excited states may contribute to relaxation.[36] However, the quadrupolar couplings predicted from nonsymmetric vibrational states tend to be much smaller than are experimentally observed for most species. As an alternative, collision–deformation models have been proposed, in which the fluctuating electric fields associated with van der Waals interactions are invoked to provide time-dependent fluctuations in the EFG.[37] In either case, the good correlation between the viscosity, temperature, and T_{1q} observed for ion pair **1a** suggests that the inverse of correlation time calculated for the BH_4^- anion using eq 3 is an appropriate estimate for anionic reorientational frequencies, at least at higher temperatures (at 223 K, some deviation from the extreme narrowing limit may be observed for spectral densities involved in determining ^{10}B and ^{11}B relaxation).

On the other hand, the $BH_4^-\{1\text{-}CH_2\}$ NOEs observed in ion pairs **1a**, **1b**, and **1c** are seen to deviate strongly from the f_{max} expected based on macroscopic viscosity and temperature. For these NOEs, it is the motion of the interionic vector $\mathbf{r}_{ii}$ which gives rise to the modulation of dipolar couplings responsible for the observed interionic NOEs (see Figure 6). Increasing aggregation of ion pairs with decreasing temperature is the most likely reason for this observation (vide supra). Aggregation will increase the average radius of the tumbling species, thereby increasing the correlation time relative to a nonaggregated species.

Anion Site Exchange and Mode Lifetimes. The final type of dynamics which will be considered is site exchange, that is, the transfer of the anion between discrete cationic sites. Multiple mechanisms for exchange can be envisioned; anion exchange could be dissociative or associative ("S_n1-like" or "S_n2-like"), could involve free ions, ion pairs or ion aggregates, and finally, might be "intramolecular" (within an aggregate) or "intermolecular" (between aggregates or ion pairs).

It is unlikely, then, that a single mechanism exists for anion exchange among the discrete cationic binding modes, and this complicates the problem of understanding the dynamics of such exchange. However, upper and lower limits on the mean lifetimes of discrete cationic binding modes can be obtained from the present data. It has already been noted that the exchange is fast on the ^1H chemical shift time scale, putting an upper limit on mean lifetimes of discrete binding modes at ca. 10^{-2}–10^{-3} s. On the other hand, the large negative deviations from expected behavior for the interionic $^1H\{^1H\}$ NOEs indicate that the *mean lifetime of a discrete ion binding mode must be greater than the correlation time of the interionic vector r_{ii}*, or else the rate of intersite exchange would predominate in determining the spectral densities relating to the interionic $^1H\{^1H\}$ NOEs. The internuclear vector between the centers of mass of the C(1) methylene protons and the BH_4^- protons shown in Figure 6 is colinear with the B–N vector, and it is the motion of this vector which is responsible for the sign and intensities of the observed interionic $^1H\{^1H\}$ NOEs. Even though the anion must be reorienting rapidly within the binding site in order to account for the observed ^{10}B and ^{11}B relaxation, the internuclear vector does not average to zero by intersite exchange rapidly enough to affect the interionic NOE. The rotational correlation time τ_{ii} of the interionic vector r_{ii} therefore provides a lower limit to the mean lifetime of a discrete ion binding mode (at least when τ_{ii} deviates from the rotational diffusion limit). By taking the maximum positive observed $BH_4^-\{1\text{-}CH_2\}$ NOE (f_{obs} at 298) as the extreme narrowing value (that is, the value which represents the maximum positive observable interionic NOE, then eq 12 may be used to obtain a value for $f_{max(T)}$ at a given temperature, where $f_{max(298)} = 0.5$.

$$f_{obs(T)}/f_{obs(298)} = f_{max(T)}/f_{max(298)} \qquad (12)$$

Equation 1 may then be used to estimate τ_{ii} at that temperature. For ion pair **1a**, this method yields τ_{ii} ranging from 1.9×10^{-11} s at 298 K to 5.9×10^{-10} s at 223 K. For **1b**, the values range from 2.8×10^{-11} s at 298 K to 7.8×10^{-10} s at 223 K, while for **1c**, the values for τ_{ii} range from 1.9×10^{-10} s at 298 K to 1.3×10^{-9} s at 223 K. The absence of any stochastic processes affecting boron relaxation with time constants of ca. 10^{-8} s sets probable limits on intersite anion exchange rates between 10^{-8} and 10^{-2} s.

Conclusions

A time-average structure for ion pairs of type **1** is described based on the analysis of interionic NOEs. Several different types of motion are identifiable in describing the dynamics of this ion pair. There is the overall motion of the ion pair (or aggregate), which is characterized by the correlation time τ_{ii}, and has a time scale ranging from 10^{-11} to 10^{-9}, depending on the temperature and size of the cation. There is anion exchange between discrete binding modes, which is faster than 10^{-2} but is slower than τ_{ii}, based on the temperature and viscosity dependence of interionic NOEs. This exchange may even be slower than 10^{-8} s, as events on this time scale should be reflected in boron relaxation, and no such effects are observed. Finally, there is the very rapid reorientation of the anion described by τ_a, which takes place on a time scale of picoseconds, and which determines the observed relaxation behavior of the boron in BH_4^-. Important motion which has as yet not been discussed is internal motion and reorientation of the cation, which is being characterized by ^{13}C and ^{15}N relaxation studies, and will be described in future publications.

Experimental Section

Sample and Solvent Preparation. Solvents used for NMR experiments were obtained from Cambridge Isotopes (Cambridge, MA). Prior to sample preparation, $^2HCCl_3$ and [$^2H_6$]dimethyl sulfoxide were passed over activated neutral alumina in order to remove traces of acid. A trace of NaO^2H was added to all ^2H_2O solutions containing BH_4^- in order to improve stability. Tetrabutylammonium tetrahydridoborate **1a** and

(33) Kowalewski, J. *Ann. Rept. NMR Spect.* **1990**, *22*, 335–343.
(34) Valiev, K. A. *Sov. Phys. JETP* **1960**, *10*, 77.
(35) Doddrell, D. M.; Bendall, M. R.; Healy, P. C.; Smith, G., Kennard, C. H. L.; Raston, C. L., White, A. H. *Aust. J. Chem.* **1979**, *32*, 1219.
(36) Brown, R. J. C.; Colpa, J. P. *J. Chem. Phys.* **1982**, *77*, 1501–1504.
(37) Osten, H. J.; Jameson, C. *J. Mol. Phys.* **1986**, *57*, 553–571.

$NaBH_4$ **2** were obtained from Aldrich, tested for purity by elemental analysis and used without further purification.

Compounds **1b** and **1c** were prepared by the method of Makosza.[38] The preparation of **1c** is given. A solution of 2.5 g of $NaBH_4$ was prepared in 20 mL of 10 N NaOH. A solution of 2 g of tetraoctylammonium bromide (Aldrich) in 15 mL of CH_2Cl_2 was shaken with 10 mL of the $NaBH_4$ solution for several minutes, after which the aqueous layer was discarded and 10 mL of fresh $NaBH_4$ solution was added and shaken for several minutes. After separation of the layers, the organic layer was dried over anhydrous sodium sulfate, filtered, and concentrated in vacuo to yield a white solid, **1c**. This material was stored under vacuum over NaOH pellets until ready for use. Product purity was monitored by comparing the integration of the BH_4^- proton resonances with that of the 1-CH_2 resonance of the cation.

NMR Spectroscopy. Samples were prepared for spectroscopy by dissolving the appropriate amounts of reagent in solvent and degassing with three freeze–thaw cycles. In cases where observed ^{10}B and ^{11}B T_1 or NOE values are compared or used to calculate predicted values, the same sample was used to obtain compared data within a 2-h time frame.

All experiments were performed either on a Varian XL-300 operating at either 300 (^1H), 32.24 (^{10}B), or 96.25 MHz (^{11}B) or on a Bruker AMX-500 operating at either 500 (^1H), 53.73 (^{10}B), and 160.42 MHz (^{11}B). Probe temperature on both instruments was controlled to within ±0.1 °C.

Spin–lattice relaxation times were measured using a standard $\pi-\tau-\pi/2$-observe sequence. Typically, 15–20 values of τ were used. Signals were integrated, and the intensities were plotted as a function of τ. T_{1obs} values were obtained by fitting of observed signal intensities to a single exponential. Because the boron signals in each case are quintets (see Figure 3), relaxation times were calculated for each line in the multiplet; however, the average value for all five lines is reported, and contributions to observed relaxation rates were calculated using those average values.

Nonselective heteronuclear NOEs were measured by presaturating all ^1H resonances of the sample with a broad band composite pulse (WALTZ-16) immediately followed by a read pulse and observation of the ^{10}B or ^{11}B free induction decay. ^1H presaturation was applied for at least five times the T_{1obs} of the boron isotope being observed, in order to insure steady state. ^1H decoupling was also applied during acquisition of the boron signal, in order to collapse the multiplet. A reference spectrum (without NOE) was obtained by ^1H decoupling during acquisition but without presaturation. The fractional enhancements reported are the differences between the NOE-enhanced signal integration (η_e) and the unenhanced integration (η_u) divided by the unenhanced integration ($f_s = (\eta_e-\eta_u)/\eta_u$)). Uncertainties in NOE measurements are estimated at ca. ±10% of the measured NOE intensity; hence, measurements of small NOEs are more precise than those of larger values. This estimate is based upon differences in measured NOE as a function of measurement variables such as changing the integral window or by comparing values obtained using cut-and-weigh methods with those obtained by electronic integration.

Selective homo- and heteronuclear NOEs were measured by presaturation of the desired resonance with low-power continuous wave irradiation for 10 s, followed by an observe pulse. Reference spectra were obtained in a similar manner, except the irradiation frequency was set to an empty region of the spectrum. NOEs were measured and reported as described above.

Viscosity and Freezing Point Depression Measurements. Solution viscosities were measured as a function of temperature for 0.2 mol/dm^{-3} solutions of **1a** in $CHCl_3$ at 295 (water bath), 281.5 (cyclohexane/liquid N_2), 262.5 (ethane diol/liquid N_2), 245 (bromobenzene/liquid N_2), and 232 K (acetonitrile/liquid N_2) as described by Crockford et al.[39] Temperature was maintained by immersion of the viscometer in the appropriate constant temperature bath. The viscosity was plotted as a function of temperature for each solution and the viscosity at the desired temperature obtained by interpolation (or extrapolation for viscosities at 223 and 298 K) of the data.

Freezing point depression measurements were made using a potentiometer equipped with twin copper/constantin thermocouples, one as the probe and the second as a reference. The reference thermocouple was immersed in an ice–water mixture. Samples of 0.2 mol/dm^3 of **1a** in $CHCl_3$ were swirled in an acetone–dry ice bath with the probe thermocouple immersed, and voltage measurements were made at 10 s intervals. Freezing was detected as a flat point in the voltage/time curve.

Acknowledgment. This work was supported in part by a grant from the NIH to Brandeis University, BRSG-S07-RR07044. T.C.P. gratefully acknowledges support through the NSF Young Investigators Program, CHE-9257036, and the Camille and Henry Dreyfus Teacher-Scholar Program. The authors thank Prof. Ernest Grunwald for his interest, stimulating discussions, and critical reading of the manuscript. They also thank Prof. A. G. Redfield for helpful discussions.

(38) Makosza, M.; Biaxecha, E. *Synth. Commun.* **1976**, *6*, 313.

(39) Crockford, H. D.; Baird, H. W.; Nowell, J. W.; Getzen, F. W. *Laboratory Manual of Physical Chemistry*, 2nd ed.; John Wiley and Sons: New York, 1975; pp 62–67..